Probing scrambling dynamics through out-of-time order correlators

Sajag Kumar[1, *]

[1] *School of Physical Sciences, National Institute of Science Education and Research.*

(Dated: April 26, 2024)

Interacting quantum systems governed by unitary dynamics (generally) thermalize. Upon thermalization any local region loses its initial information. Scrambling dynamics describes the flow of this *lost* information to non-local degrees of freedom. It can be characterised by the growth of local Heisenberg operators. The out-of-time order correlator (OTOC) allows us to measure this spread of operators. Recently, due to a bound on the growth of OTOCs in certain systems, and a realisation that a spin system (SYK model) and (holographic dual of) black holes saturate this bound, has led to a number of studies on the behaviour of OTOC in various quantum and classical systems. For short-range interacting quantum many-body systems the Lieb-Robinson bound describes the lightcone of the OTOC. However, the behaviour of OTOC in long-range systems is still poorly understood. In this project, we numerically compute the OTOC (or the decorrelator in the classical limit) for various classical (Kauffman cellular automaton (KCA) and classical Ising model) and quantum systems (the transverse field Ising model). For the simulations we have used the monte carlo method (KCA), finite element and Runge-Kutta (RK4) method (classical Ising model), and tensor networks (transverse field Ising model).

INTRODUCTION

Imagine a quantum spin chain of interacting spin-1/2 particles. Consider two orthogonal initial pure states of the chain, which have approximately the same average energy but opposite expectation values for σ^z (the magnetisation in z direction). If the system is chaotic, and if we consider the time evolution of these two states at a time long enough times, the expectation value of the operator will be approximately the same in both time-evolved states. This is called thermalization. Upon thermalization the expectation value of this operator matches the expectation value of the thermal density matrix with the energy of the initial states. These two states look the same at late times as far as the measurements of these operators are concerned. Information seem to have lost from the local degree of freedom to the non-local degrees of freedom (assuming the system is closed). Quantum information scrambling is the study of this flow of information from local to non-local degrees of freedom.

The flow of information to non-local degrees of freedom is characterised by the spreading of local operators. An out-of-time order correlator allows us to measure this spread of operators. The idea is to probe the spread of $W(t)$ with another operator V, which is localised at some distance away from $W(0)$.

Out-of-time order correlator

In the setting of quantum many-body spin systems, the out-of-time order correlator is defined as

$$\langle W(x,t)V(0,0)\rangle \tag{1}$$

where $W(x,t)$ and $V(0,0)$ are Hermitian operators localised around x at time $t = t$ and around 0 at time $t = 0$, respectively. The OTOC is a measure of the effect of $V(0,0)$ on the measurement of the operator $W(x,t)$. This is clearly seen once we look at this correlator as the inner product of the following states

$$|\psi_1\rangle = W(x,t)V(0,0)\,|\phi\rangle \tag{2}$$
$$= e^{\iota Ht}W(x,t)e^{-\iota Ht}V(0,0)\,|\phi\rangle \tag{3}$$

and

$$|\psi_2\rangle = V(0,0)W(x,t)\,|\phi\rangle \tag{4}$$
$$= V(0,0)e^{\iota Ht}W(x,t)e^{-\iota Ht}\,|\phi\rangle \tag{5}$$

the decorrelator is just the inner product of these two states. If the action of $V(0,0)$ has no effect then this quantity should be one, otherwise depending on the action of $V(0,0)$ it takes an intermediate value between 0 and 1.

The classical limit of the OTOC

In quantum mechanics the out-of-time order commutator between two Hermitian operators is given by

$$\langle [W(x,t)V(0,0)]^2\rangle. \tag{6}$$

In the setting of classical spin systems an analogous expression can be written for the decorrelator between two copies of classical spin systems is given by

$$D(x,t) = \langle \mathbf{S}_i^A(t), mathbf S_0^B(0)\rangle \tag{7}$$

where A and B denote the two copies is the Poisson bracket and $\langle\rangle$ denotes average over the thermal Gaussian ensemble. One can simplify this further to obtain

$$D(x,t) = \frac{1}{2}(1 - \langle \mathbf{S}_x^A(t)\cdot \mathbf{S}_x^B(t)\rangle) \tag{8}$$

this is the classical limit of the OTOC called the decorrelator.

We have followed [1], [2] for the discussion on OTOCs and quantum information scrambling.

In the following sections we first compute the decorrelator for two classical systems, Kauffman cellular automaton, and classical spins on a one-dimensional lattice. We compare the decorrelator for different models and various parameters. Then, we give a brief review of matrix product states and algorithms for time evolution of matrix product states. Following which we compute the OTOC for the transverse field Ising model, and similar models with more than just nearest neighbour interaction. For the tensor network calculations in the quantum case we use *TenPy* library [3].

KAUFFMAN CELLULAR AUTOMATON

A cellular automaton is a model of computation. It is a collection of cells arranged in some specific geometry. Each cell is assigned a state from the state space and the evolution of this state in time is governed by a set of local rules. We study the Kauffmann cellular automaton (KCA) motivated by [4]. The KCA is a system of N cells in one dimension. The state ($\sigma(r,t)$) of a certain cell at time t and position r can be ± 1. Time evolution of the system is governed by a set of local rules $f_{r,t}$:

$$\sigma(r,t+1) = f_{r,t}[\sigma(r-K,t),...,\sigma(r,t),...,\sigma(r+K,t)]. \quad (9)$$

which are random with probability p in space and time, $f_{r,t}$ is 1 with probability p and -1 with probability $1-p$. The future state of a cell depends on the local rules and its $2K+1$ neighbouring cells.

We want to study how quickly does the knowledge of the state of a cell propagates through the automaton. We do this by computing the OTOC which in the case of the KCA is:

$$d(r,t) = \frac{1}{2}[1 - \langle \sigma^A(r,t)\sigma^B(r,t)\rangle_p] \quad (10)$$

where σ^A and $sigma^B$ are the states of two copies of KCA which at $t=0$ only differ in the state of cell at $r=0$, the $\langle\rangle_p$ represents ensemble average over realisations with the same p. The classical OTOC is just the local distance between the systems A and B. We obtain the OTOC for various values of K as shown in figure 1 and 2, in particular we observe that for high values of p the dynamics of the KCA is chaotic while it is not the case for smaller values.

Simulation details. For our simulations we choose $N = 2048$, $t = 400$ and $p = 0.40$ (except in figure 1(b)). The initial state is generated randomly by choosing one among ± 1 with probability 0.5. We update the local rules after each time step. The ensemble average is done over (100, 100, 500, 25, 20) realisations for $K = (2, 3, 4, 5, 6)$. For figure 1(b) we average over 100 realisations of the initial state. The random numbers were generated with *NumPy*.

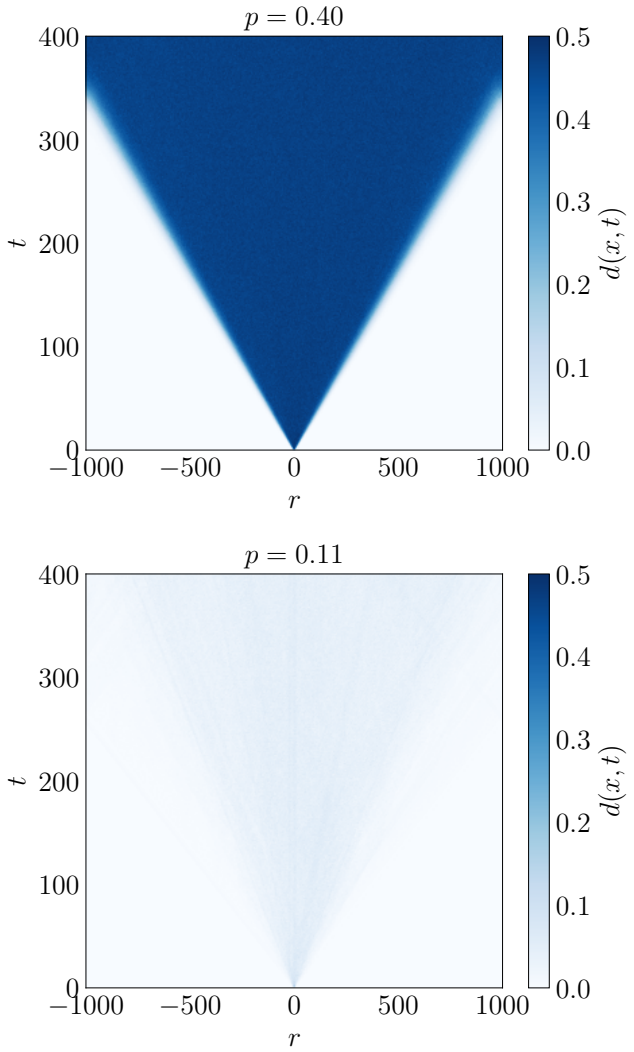

FIG. 1. Lightcone structure of the decorrelator $d(r,t)$ with $N = 2048$ and $K = 4$,with a single spin flip at the origin $r = 0$ when $t = 0$. (Top) For $p = 0.40$ we obtain the expected behaviour where the initial perturbation spreads through the system with a linear wavefront. (Bottom) Once we increase the bias of the local rules towards one of the values the perturbation freezes. When $p = 0.11$ the perturbation barely spreads through the system. The very faint lightcone like structure is an artifact of averaging over less number of automatons and will vanish once we sample a large number of automatons.

CLASSICAL SPIN SYSTEMS

In this section we consider classical spins on a one dimensional lattice motivated by [5]. Classical spins are

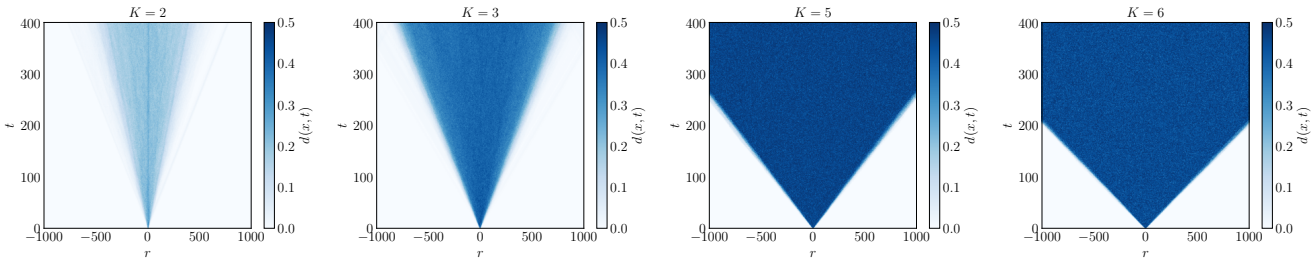

FIG. 2. Comparison of the lightcone structure of the decorrelator for different values of K. The perturbation spreads with a velocity directly proportional to K. This is expected, as K determines the number of neighbouring cells whose states govern the dynamics of a certain cell. The velocity of perturbations (or the boundary of the lightcone) may not be captured well in these figures. precise boundaries may be obtained by averaging over a large number of automatons.

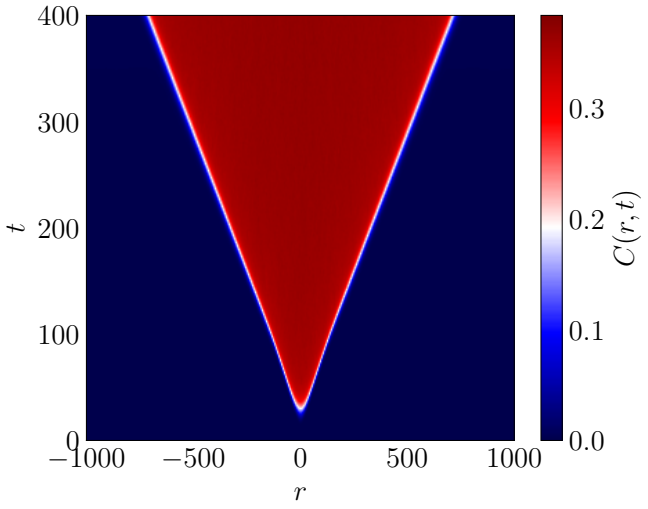

FIG. 3. Lightcone structure of the decorrelator for the classical Ising chain with nearest neighbour interactions whose dynamics is governed by the Hamiltonian in (11). The decorrelator is obtained for two infinite temperature copies of the system which are same at $t = 0$ but in the polar angle of the spin at site $r = 0$ (they differ by $\epsilon = 0.001$). A sharp boundary is observed between correlated and uncorrelated spins. This small initial perturbation drives the two systems away from each other in the phase space. After some time ($t > 400$), the two systems will be completely decorrelated. This is the hallmark of chaos.

unit vectors in three dimensions. A classical spin is obtained by taking the $S \to \infty$ limit of a spin-S quantum spin. These classical systems are studied with the motivation to decipher the behaviour of large spin quantum systems.

We take the well studied classical many-body model the classical Ising model with nearest neighbour interactions. The model is described by the Hamiltonian in 11.

$$\mathcal{H}_1 = -J \sum_{i=0}^{N-1} \mathbf{S_i} \cdot \mathbf{S_{i+1}} \tag{11}$$

We want to study how the knowledge of a small perturbation spreads through the system. We do so by the following protocol. We take two copies of an infinite temperature state, and we slightly rotate one of the spins by an angle ϵ, and follow the trajectory of both the copies in phase space. The measure of how far they are in phase space is given by the classical OTOC or the decorrelator

$$D(r,t) = \frac{1}{2}(1 - \langle \mathbf{S}_r^a(t) \cdot \mathbf{S}_r^b(t) \rangle) \tag{12}$$

where a and b represent the two copies, the average is over noisy infinite temperature initial states. When and where two spins are correlated the decorrelator is 0 and when and where they are uncorrelated the decorrelator is 1. We obtain a lightcone structure for the decorrelator as shown in figure 3. The knowledge of the local perturbation spreads linearly in time through the system.

We further explore this model by adding next and next-nest nearest model interaction to the classical Ising model. The model with next-nearest neighbour interaction is governed by the Hamiltonian $\mathcal{H}_2$ given by

$$\mathcal{H}_2 = -J_1 \sum_{i=0}^{N-1} \mathbf{S_i} \cdot \mathbf{S_{i+1}} - J_2 \sum_{i=0}^{N-1} \mathbf{S_i} \cdot \mathbf{S_{i+2}} \tag{13}$$

while the model with next-next nearest neighbour interaction as well is governed by $\mathcal{H}_3$ which is as follows

$$\mathcal{H}_3 = -\sum_{i=0}^{N-1} \left(J_1 \mathbf{S_i} \cdot \mathbf{S_{i+1}} + J_2 \mathbf{S_i} \cdot \mathbf{S_{i+2}} + J_3 \mathbf{S_i} \cdot \mathbf{S_{i+3}}\right). \tag{14}$$

We compute the spin dynamics by integrating the standard equations of motion $\partial_t S_i = \{S_i, H\}$, where $\{\ldots\}$ indicate Poisson brackets, and the spins S_i satisfy the

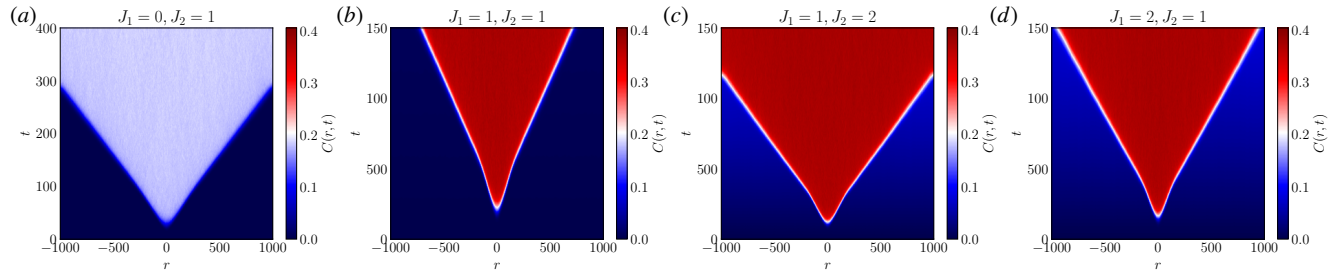

FIG. 4. Lightcone structures for the J_1-J_2 classical Ising model. The dynamics of the model is governed by the Hamiltonian in (13). The protocol for computing the decorrelator is same as in the nearest-neighbour model. (a) Only next-nearest neighbours (nnn) interact, the nearest neighbour (nn) interaction strength is set to 0. The perturbation spreads weakly, there is a lightcone structure to the spread but even the spins inside the lightcone seem sufficiently uncorrelated. (b) $J_1 = J_2$ i.e. both interaction strength are the same. The perturbation spreads with a velocity larger than in the case of nearest neighbour model. Which is the expected behavior similar to the Kauffman cellular automaton, where all the K neighbours interacted with equal strength. We study two other cases, (c) $2J_1 = J_2$ and (d) $J_1 = 2J_2$, in both the cases the lightcone structure is present with velocity of the perturbation even higher than in (b). However, in these models there is no sharp boundary between correlated and uncorrelated spins. Once again this behaviour may vanish upon averaging over a large number of initial states but all the simulations here sample over a fixed number of states. So there is a chance that this is the true behaviour of the model.

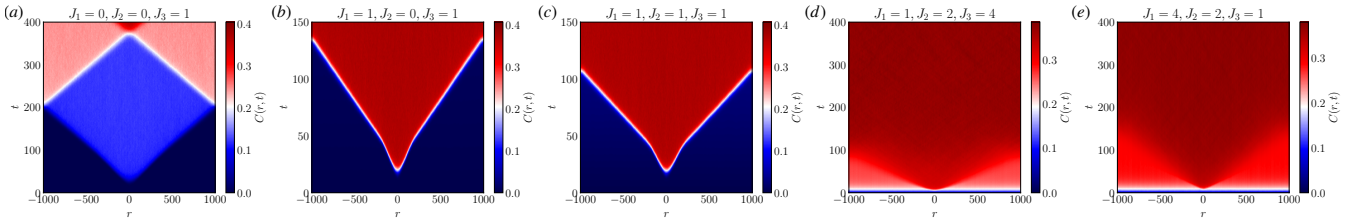

FIG. 5. Lightcone structures for the J_1-J_2-J_3 classical Ising model. The dynamics of the model is governed by the Hamiltonian in (13). The protocol for computing the decorrelator remains the same. We tune the interaction strength between nearest, next-nearest and next-next-nearest neighbours and compare the resulting lightcone structure. (a) When we have only next-next-nearest neighbour interactions, a highly non-trivial structure in the lightcone emerges with different regimes of fixed value of the decorrelator separated by sharp boundaries. It is highly unlikely that this structure will vanish upon averaging over a large number of initial states. In case there is (b) no next-nearest neighbour interaction or (c) all the interactions are equally strong, the typical lightcone structure with a sharp boundary is obtained is obtained. The observed boundary for these models is not linear. We study two more models, as an extension of the $J_1 = 2J_2$ and $2J_1 = J_2$ models, with (d) $J_1 = 2J_2 = 4J_3$ and (e) $J_3 = 2J_2 = 4J_1$, in both these cases the systems decorrelates very quickly. The lightcone structure is still present but without a sharp boundary.

relation $\{S_i^\alpha, S_{i'}^\beta\} = \delta_{ii'}\varepsilon^{\alpha\beta\gamma}S_i^\gamma$. The equation of motion for the system governed by the Hamiltonian $\mathcal{H}_1$ is,

$$\frac{d\mathbf{S}_i}{dt} = J\mathbf{S}_i \times (\mathbf{S}_{i-1} + \mathbf{S}_{i+1}), \tag{15}$$

for $\mathcal{H}_2$ is,

$$\frac{d\mathbf{S}_i}{dt} = J_1\mathbf{S}_i \times (\mathbf{S}_{i-1} + \mathbf{S}_{i+1}) + \tag{16}$$

$$J_2\mathbf{S}_i \times (\mathbf{S}_{i-2} + \mathbf{S}_{i+2}), \tag{17}$$

and finally for $\mathcal{H}_3$ is,

$$\frac{d\mathbf{S}_i}{dt} = J_1\mathbf{S}_i \times (\mathbf{S}_{i-1} + \mathbf{S}_{i+1}) + \tag{18}$$

$$J_2\mathbf{S}_i \times (\mathbf{S}_{i-2} + \mathbf{S}_{i+2}) + \tag{19}$$

$$J_3\mathbf{S}_i \times (\mathbf{S}_{i-3} + \mathbf{S}_{i+3}). \tag{20}$$

The results of the decorrelator computation for these models is shown in figure 4 and 5. The lightcone structure of the decorrelator emerges in all the cases. The perturbation velocity, as expected depends on the strength and range of the interaction. The cases with only next-nearest and only next-next nearest neighbour interaction are interesting. With the perturbation spreading very slowing in one and a complicated structure of the lightcone in the other. Also for the next-next nearest model the Lieb-Robinson bound does not seem to hold, with the perturbation spreading almost instantaneously through the system. This is not a problem however as the Lieb-Robinson bound holds only for quantum systems.

Simulation details. For our simulations we take 2048 spins on a one-dimensional lattice and evolve them for 400 seconds. We solve the equations of motion using two different methods. Firstly, we tried finite element

method. We obtained correct solutions but the time step chosen had to kept smaller than 0.001 seconds which led to a huge grid for our choice of the system size and evolution time. We then moved to Runge-Kutta method (RK4), where we could do the simulations with a time step of 0.1 seconds. To generate infinite temperature initial states we generate an array of random numbers between 0 and 2π and use them as the polar and azimuthal angles of the spins. To introduce the perturbation we increase the polar angle of the spin at site 0 by $\epsilon = 0.001$ radians. The interaction strengths parameters are indicated in the corresponding figures. We average over 1000 initial state realisations for figures 4 and 5, and over 5000 realisations of the initial state for 3.

MATRIX PRODUCT STATES

The ground state of local Hamiltonians follow and area law of entanglement entropy. The entanglement entropy of a generic bipartition scales as the boundary of one of the two regions. A matrix product state is an ansatz for the ground state of such a Hamiltonian in one dimension. In Penrose's tensor network notation, a matrix product state is

$|\Psi\rangle =$ 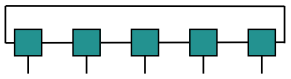 . (21)

We are going to use this notation in rest of the discussion, the block are tensors and the legs are the indices. For example the inner product between two MPS is given by

$\langle\Psi]|\Psi\rangle =$ 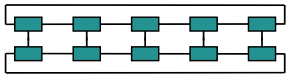 . (22)

TIME EVOLUTION OF MATRIX PRODUCT STATES

The time evolution of a quantum state under a Hamiltonian H is given by

$$U(\delta t)\,|\Psi\rangle = e^{-\iota H \delta t}\,|\Psi\rangle \tag{23}$$

where δt is the time step, we have set $\hbar = 1$. This is just a matrix exponentiation. Once we have the time evolution matrix we can act it on the state to obtain the time evolved state. However for many body systems the Hilbert space dimension and hence the dimension of the Hamiltonian grows as 2^{2N}, where N is the number of particles in the system. This makes the Hamiltonian extremely large for even small systems. Computing the eigenvalues and eigenvectors of such a large matrix is not possible for current computers. The exponentiation of such a large matrix remains intractable even for very efficient sparse matrix inversion algorithms. In the following section we review two approaches to time evolution of matrix product states.

Time Evolving Block Decimation

Time evolving block decimation (TEBD) is an algorithm that approximates $U(\delta t)$. This algorithm works well for short range interacting systems. The main idea behind the algorithm is to write

$$U(\delta t) = e^{-\iota H_1 \delta t} e^{-\iota H_2 \delta t}\,|\Psi\rangle \tag{24}$$

where $H = H_1 + H_2$ is the original Hamiltonian. Note that this can be done, if H_1 and H_2 commute. Consider an MPS as discussed in the previous section and an MPO (matrix product operator) of the system's Hamiltonian, using the above prescription we contract appropriate terms of the MPO, with the action of the Hamiltonian on the MPS reduced to

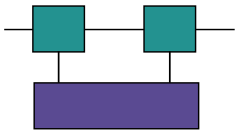 , (25)

we contract the indices to obtain a rank four tensor

 , (26)

which can we support vector decomposed to

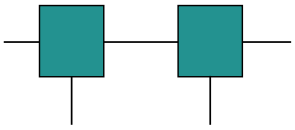 , (27)

which is an MPS. So we have obtained the time evolution of an MPS and also managed to retain its tensor network structure.

Time Dependent Variational Principle

In the time dependent variational principle we do not calculate the matrix exponential but rather the action of $U(\delta t)$ on $|\Psi\rangle$ directly. The main idea behind the algorithm is to variationally minimise the the distance between $H\,|\Psi\rangle$ and $|\partial_t \Psi\rangle$, i.e. an MPS and an MPS in

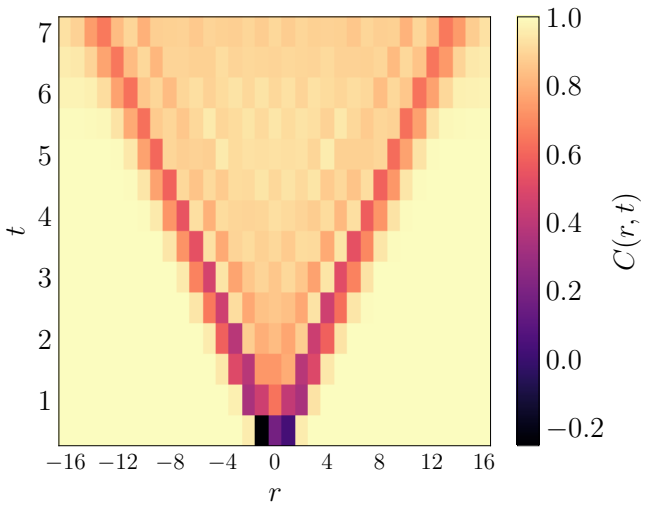

FIG. 6. Lightcone structure of the out-of-time order correlator for the transverse field Ising model with only nearest neighbour interaction. The time evolving block decimation algorithm was used for this calculation. A clear lightcone boundary is observed. The boundary is linear. This is in accordance with the Lieb-Robinson bound in short-range quantum spin systems. The values of the OTOC inside the lightcone however is a bit puzzling, it appears as if lost information is recovered after sometime. It is highly likely that this will vanish upon averaging over many initial state realizations.

its tangent space. In the tensor network language one component of this equation that can be solved exactly is written as

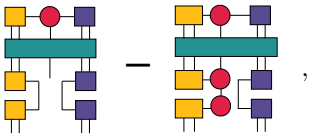

(28)

where the blue block is the Hamiltonian and the top blocks on top of the Hamiltonian is the MPS in its canonical form. The canonical form of an MPS is the when one part of the MPS is left normalised and the other part is right normalised, with an active site separating the two parts. The active site in not normalised. The solution of this equation gives the time evolved state in the tangent space of the initial MPS.

In the preceding two sections we have followed the discussion in [6] and the book 'Principles of Quantum Computation and Information' by Benenti, Casati, Rossini and Strini.

TRAVERSE FIELD ISING MODEL

The motivation for this project was to understand the OTOC lightcone in long-range interacting quantum systems. In the previous sections we have seen the behaviour of the decorrelator in short-range classical systems. We expect a similar behaviour for a short-range quantum system. For classical spin systems our model of choice was the nearest neighbour Ising model. For quantum spin systems our model of choice is going to be the transverse field Ising model. The model Hamiltonian is

$$H = -J \sum_{i=0}^{N-1} \sigma_i^x \sigma_{i+1}^x - g \sum_{i=0}^{N-1} \sigma_i^z \tag{29}$$

where J and g are the nearest neighbour and magnetic field interaction strengths, respectively. Note that this is the simplest possible interacting quantum spin model. Removing g from this model does not work as the corresponding model does not evolve in time.

To study the lightcone in long-range quantum systems, we take a naive approach. We increase the interaction range of the model one spin at a time. In particular, we study two models with next-nearest and next-next nearest neighbour interactions. The Hamiltonian for next-nearest model is

$$H_2 = -\sum_{i=0}^{N-1} \left(J_1 \sigma_i^x \sigma_{i+1}^x + J_2 \sigma_i^x \sigma_{i+2}^x \right) - g \sum_{i=0}^{N-1} \sigma_i^z \tag{30}$$

and the next-next nearest model is

$$H_3 = -\sum_{i=0}^{N-1} \left(J_1 \sigma_i^x \sigma_{i+1}^x + J_2 \sigma_i^x \sigma_{i+2}^x + J_3 \sigma_i^x \sigma_{i+3}^x \right) \tag{31}$$

$$- g \sum_{i=0}^{N-1} \sigma_i^z. \tag{32}$$

We compute the $\sigma^z\sigma^z$ OTOC given by

$$C(r,t) = \langle \Psi | \, \sigma_r^z(t) \sigma_0^z(0) \sigma_r^z(t) \sigma_0^z(0) \, | \Psi \rangle \tag{33}$$

where $\sigma_r^z(t)$ is the time evolved local Heisenberg operator at site r at time t and $\sigma_0^z(0)$ is the local operator at site 0 at $t = 0$. The results are shown in figure 6 and 7. The lightcone structure for the next-nearest and next-next nearest models are as expected. However, for the nearest neighbour model the obtained results seem to indicate similar behaviour inside and outside the boundary of the lightcone. It appears as if there is no information scrambling inside the lightcone boundary. This might as well be a result of not averaging over many realisations of the initial state.

Simulation details. We use TEBD and TDVP for the nearest neighbour model. For the next and next-nearest neighbour models we only use TDVP. *TenPy* library is used for all the calculations. One hindrance is that there is no way of computing the time evolution of an operator in this library. So to compute the OTOC we first initialise an MPS in ferromagnetic configuration. We make two copies of this MPS. Then on one of the copies we apply $\sigma_0^z(0)$ to the MPS. This state is evolved backwards in

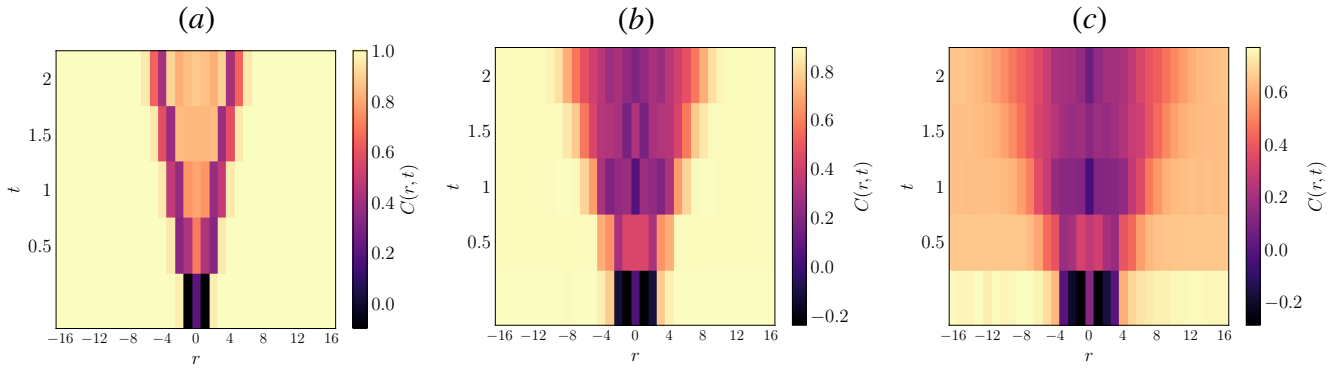

FIG. 7. The lightcone structure of the OTOC using time-dependent variational principle. (a) For the nearest neighbour model as described by H. This is in accordance with the results obtained for the TEBD case. (b) For the next-nearest neighbour model as described by H_2, the lightcone structure emerges with a higher velocity than in the nearest neighbour case. The boundary remains linear. (c) For the next-next nearest neighbour model as described by H_3. The lightcone boundaries are already flat for 33 spins. To understand the lightcone better we need to do the simulation for larger number of spins but it is highly unlikely that the lightcone boundary would be linear.

time. $\sigma_r(0)$ is applied on the backward evolved state. This state is then forward evolved in time by and equal amount. Say this copy was $|\psi\rangle$ so the procedure described above yields

$$e^{\iota Ht}\sigma_r^z(0)e^{-\iota Ht}\sigma_0^z(0)\,|\psi\rangle\,. \tag{34}$$

We first evolve the other copy backwards in time, then apply $\sigma_r^z(0)$, forward evolve this state for the same time and finally apply $\sigma_0^z(0)$ on it. Say this copy was $|phi\rangle$, then the above procedure yields

$$\sigma_0^z(0)e^{\iota Ht}\sigma_r^z(0)e^{-\iota Ht}\,|\phi\rangle \tag{35}$$

The OTOC is then just the inner product of these two states

$$C(r,t) = \langle\phi|\psi\rangle\,. \tag{36}$$

We consider 33 spins-1/2 particles on a 1D lattice. We evolve the system for 7.5 seconds in case of nearest neighbour model with TEBD and for 2.5 seconds in case of TDVP. For both the TDVP and TEBD simulations we take a time steps of 0.5 seconds. We set all the interaction strength parameters to 1 in all of our simulations. The truncation parameters for both TEBD and TDVP are the same. We use a maximum bond dimension of 100 and error threshold during SVD decomposition was set to 10^{-12}. We use the two site TDVP engine for our simulations. We do not average over initial state realisations.

SUMMARY AND OUTLOOK

We studied the dynamics of the decorrelator in Kauffman cellular automaton using Monte Carlo simulations. It was observed that the velocity of the perturbation depends on the number of neighbours responsible for time evolution. Also different regimes of dynamics was obtained for high and low p. We then moved on to study the effect of local perturbations in classical spin systems. We integrated the equations of motion using Runge-Kutta (RK4) and finite element method. To go beyond nearest neighbour interaction we systematically add next and next-next nearest neighbour interaction to our Hamiltonian. We compute the decorrelator for various combinations of interaction strength parameters. We obtain lightcone structure in the decorrelator of all of these systems. This highlights that even though there is no classical Lieb-Robinson bound, there is still an emergent Lieb-Robinson bound on the velocity of perturbations in classical systems. This emergent bound seem to vanish with increasing interaction range and strength. For quantum spin systems, in close analogy with our analysis of classical spin systems, we chose the transverse field Ising model for our study. Just like in the classical case we systematically added next and next-next nearest interaction to the system. We computed the $\sigma^z\sigma^z$ OTOC for these models. We use both TEBD and TDVP algorithm for the nearest neighbour case. For the other models we only use TDVP. We see the OTOC lightcone emerging in these systems. It was observed that the operator spreading was fastest in the next-next nearest neighbour model while the slowest in the nearest neighbour model. We could not play around with the interaction strength parameters of these models as each lightcone computation is very expensive. In our approach we have to do the time evolution for each point of the grid. In fact all of our simulations suffer from the problem of being very slow. In case of Monte Carlo simulations while the individual steps are quick we have to average over a large number of initial

realisations to obtain good results, which becomes expensive, parallelising this computation would require a good GPU for efficient implementation. Even the *TenPy* codes are optimised for GPU implementation. Further for the quantum simulations instead of time evolving the MPS we could instead time evolve the MPO. This would make the OTOC computations much quicker. There are dedicated algorithms for MPO evoution including TEBD and TDVP versions for MPO [7]. With better computational resources it would be nice to explore the transverse field Ising model with further interactions and different interaction parameters. In particular corresponding to the parameters which show non-trivial behaviour in the classical regime. It would also be nice to compare and contrast classical and quantum information scrambling.

Acknowledgements. Prof. Anamitra Mukherjee for suggesting the problem. Prof. Subhasish Basak for the computational physics course. The SPS computer center, where all the codes were executed. Deepak, Jabed and Sagar for company at the computer center during the runtime of the codes.

* sajag.kumar@niser.ac.in

[1] B. Swingle, Nature Physics **14**, 988 (2018).
[2] S. Xu and B. Swingle, PRX Quantum **5**, 010201 (2024), 2202.07060.
[3] J. Hauschild and F. Pollmann, SciPost Phys. Lect. Notes 5 (2018) (2018), 10.21468/SciPostPhysLectNotes.5, 1805.00055.
[4] S. Liu, J. Willsher, T. Bilitewski, J. Li, A. Smith, K. Christensen, R. Moessner, and J. Knolle, Phys. Rev. B **103**, 094109 (2021), 2101.01313.
[5] A. Das, S. Chakrabarty, A. Dhar, A. Kundu, D. A. Huse, R. Moessner, S. S. Ray, and S. Bhattacharjee, Phys. Rev. Lett. **121**, 024101 (2018), 1711.07505.
[6] S. Paeckel, T. Köhler, A. Swoboda, S. R. Manmana, U. Schollwöck, and C. Hubig, Annals of Physics **411**, 167998 (2019), 1901.05824.
[7] S. Xu and B. Swingle, Nat. Phys. **16**, 199 (2020), 1802.00801.